Kinetics and Mechanism for Reversible Chloride Transfer between Mercury(II) and Square-Planar Platinum(II) Chloro Ammine, Aqua, and Sulfoxide Complexes. Stabilities, Spectra, and Reactivities of Transient Metal−Metal Bonded Platinum−Mercury Adducts

Östen Gröning,[†] Alan M. Sargeson,[‡] Robert J. Deeth,[§] and Lars I. Elding*[,†]

Inorganic Chemistry 1, Chemical Center, University of Lund, P.O. Box 124, SE-221 00 Lund, Sweden, Research School of Chemistry, The Australian National University, Canberra, ACT 0200, Australia, and Department of Chemistry, University of Warwick, Coventry, CV4 7AL, U.K.

Received March 24, 2000

The Hg^{2+}_{aq}- and $HgCl^{+}_{aq}$-assisted aquations of $[PtCl_4]^{2-}$ (**1**), $[PtCl_3(H_2O)]^-$ (**2**), *cis*-$[PtCl_2(H_2O)_2]$ (**3**), *trans*-$[PtCl_2(H_2O)_2]$ (**4**), $[PtCl(H_2O)_3]^+$ (**5**), $[PtCl_3Me_2SO]^-$ (**6**), *trans*-$[PtCl_2(H_2O)Me_2SO]$ (**7**), *cis*-$[PtCl(H_2O)_2Me_2SO]^+$ (**8**), *trans*-$[PtCl(H_2O)_2Me_2SO]^+$ (**9**), *trans*-$[PtCl_2(NH_3)_2]$ (**10**), and *cis*-$[PtCl_2(NH_3)_2]$ (**11**) have been studied at 25.0 °C in a 1.00 M $HClO_4$ medium buffered with chloride, using stopped-flow and conventional spectrophotometry. Saturation kinetics and instantaneous, large UV/vis spectral changes on mixing solutions of platinum complex and mercury are ascribed to formation of transient adducts between Hg^{2+} and several of the platinum complexes. Depending on the limiting rate constants, these adducts are observed for a few milliseconds to a few minutes. Thermodynamic and kinetics data together with the UV/vis spectral changes and DFT calculations indicate that their structures are characterized by axial coordination of Hg to Pt with remarkably short metal−metal bonds. Stability constants for the Hg^{2+} adducts with complexes **1**−**6**, **10**, and **11** are $(2.1 \pm 0.4) \times 10^4$, $(8 \pm 1) \times 10^2$, 94 ± 6, 13 ± 2, 5 ± 2, 60 ± 6, 387 ± 2, and 190 ± 3 M^{-1}, respectively, whereas adduct formation with the sulfoxide complexes **7**−**9** is too weak to be observed. For analogous platinum(II) complexes, the stabilities of the Pt−Hg adducts increase in the order sulfoxide ≪ aqua < ammine complex, reflecting a sensitivity to the π-acid strength of the Pt ligands. Rate constants for chloride transfer from $HgCl^+$ and $HgCl_2$ to complexes **1**−**11** have been determined. Second-order rate constants for activation by Hg^{2+} are practically the same as those for activation by $HgCl^+$ for each of the platinum complexes studied, yet resolved contributions for Hg^{2+} and $HgCl^+$ reveal that the latter does not form dinuclear adducts of any significant stability. The overall experimental evidence is consistent with a mechanism in which the accumulated Pt(II)−Hg^{2+} adducts are not reactive intermediates along the reaction coordinate. The aquation process occurs via weaker Pt−Cl−Hg or Pt−Cl−HgCl bridged complexes.

Introduction

Metal-assisted hydrolysis is well-known for octahedral complexes and has been reviewed.[1] In particular, mercury(II)-promoted reactions of octahedral halide transition metal complexes have been extensively studied. The mechanism usually proposed for these reactions involves rapid formation of an M−X−Hg bridged intermediate followed by a rate-determining cleavage of the M−X bond.[1] Occasionally, saturation kinetics have been observed and attributed to formation of halide-bridged intermediates. These reactions have been perceived as essentially dissociative, and evidence of 5-coordinate intermediates has been obtained.[1] In general terms, they can be regarded as chloride transfer processes to mercury(II) from another metal center.

Hydrolysis of square-planar halide complexes is also activated by Hg^{2+} ion, and halide abstraction by the use of Hg(II) and Ag(I) is an established method for preparation of solvento complexes.[2,3] However, except for early studies of the mercury(II)-assisted aquation of [Pt(glycine)(NH_3)X], X = Cl, Br,[4,5] and a few investigations of metal ion activated hydrolysis of cisplatin and some sterically hindered palladium complexes,[6−9] no quantitative mechanistic investigations of metal-assisted square-planar substitutions seem to have been published. The interpretation of the data in the few previous studies of square-planar systems conform to the halide bridge mechanism generally used for octahedral systems.[1]

In a study of some mercury(II)-promoted chloride transfer reactions of platinum(II) complexes we observed more complex behavior, not immediately compatible with the simple bridge mechanism. In order to elucidate the mechanism for these reactions in more detail, we have performed a systematic study of the mercury(II)-assisted hydrolysis of the following com-

[†] University of Lund.
[‡] The Australian National University.
[§] University of Warwick.

(1) Banerjee, R. *Coord. Chem. Rev.* **1985**, *68*, 145.
(2) Davies, J. A.; Hockensmith, C. M.; Kukushkin, V. Yu.; Kukushkin, Yu. N. *Synthetic Coordination Chemistry*; World Scientific: Singapore, 1996, Chapter 3.
(3) Elding, L. I. *Inorg. Chim. Acta* **1976**, *20*, 65.
(4) Venediktov, A. B.; Belyaev, A. V. *Izv. Sib. Otd. Akad. Nauk SSSR, Ser. Khim. Nauk* **1974**, 51.
(5) Venediktov, A. B.; Belyaev, A. V. *Izv. Sib. Otd. Akad. Nauk SSSR, Ser. Khim. Nauk* **1975**, 67.
(6) Cusumano, M.; Guglielmo, G.; Ricevuto, V.; Romeo, R.; Trozzi, M. *Inorg. Chim. Acta* **1976**, *17*, 45.
(7) Guglielmo, G.; Ricevuto, V.*Chim. Ind.* (*Milan*) **1976**, *58*, 655.
(8) Cusumano, M.; Guglielmo, G.; Marricci, P.; Ricevuto, V. *Inorg. Chim. Acta* **1978**, *30*, 29.
(9) Miller, S.; Wen, H.; House, D. A.; Robinson, W. T. *Inorg. Chim. Acta* **1991**, *184*, 111.

10.1021/ic000320j CCC: $19.00
Published on Web 08/23/2000

plexes: $[PtCl_4]^{2-}$ (**1**), $[PtCl_3(H_2O)]^-$ (**2**), *cis*-$[PtCl_2(H_2O)_2]$ (**3**), *trans*-$[PtCl_2(H_2O)_2]$ (**4**), $[PtCl(H_2O)_3]^+$ (**5**), $[PtCl_3Me_2SO]^-$ (**6**), *trans*-$[PtCl_2(H_2O)Me_2SO]$ (**7**), *cis*-$[PtCl(H_2O)_2Me_2SO]^+$ (**8**), *trans*-$[PtCl(H_2O)_2Me_2SO]^+$ (**9**), *trans*-$[PtCl_2(NH_3)_2]$ (**10**), and *cis*-$[PtCl_2(NH_3)_2]$ (**11**). Kinetics and transient UV/vis spectra have been recorded in media containing variable concentrations of chloride in order to resolve the contributions from Hg^{2+}, $HgCl^+$, and $HgCl_2$.

Saturation kinetics and very large UV/vis spectral changes occurring instantaneously on mixing solutions of mercury(II) and platinum complex indicate the formation of thermodynamically stable but short-lived complexes between Hg^{2+} and several of the platinum(II) complexes. A transient adduct between Hg^{2+} and platinum(II) has been reported in one case before, namely, for [Pt(glycine)(NH_3)X].[10] Moreover, the spectra and thermodynamic properties of the adducts are not compatible with a simple chloride-bridged Pt−Cl−Hg structure, but rather with a direct Pt−Hg interaction. Recent interest in metal−metal interactions has revealed several d^8−d^{10} metal−metal bonded compounds which may serve as models for such species.[11] For example, a direct Pt(II)−Tl(III) bond unassisted by bridges has been detected in aqueous cyanide solutions of $[(Pt(CN)_4]^{2-}$ and Tl(III),[12] and $[Tl_2Pt(CN)_4]$ has been characterized in the solid state.[13] There are also examples where bridging ligands assist the stabilization of the metal−metal bond.[14,15] Thus, a range of structures should be considered as possible candidates for the transient platinum−mercury adducts formed in the present systems. In order to further elucidate these structures, UV/vis spectra have been analyzed and density functional computations have been performed.

Experimental Section

Chemicals and Solutions. *cis*- and *trans*-$[PtCl_2(NH_3)_2]$ (Sigma) were used without further purification. Solutions of $[PtCl_4]^{2-}$ were prepared immediately before use from the solid potassium salt (Johnson and Matthey). Solutions of $[PtCl_3(H_2O)]^-$, *trans*-$[PtCl_2(H_2O)_2]$, $[PtCl_3Me_2SO]^-$, and $[Pt(H_2O)_3Me_2SO]^{2+}$ were prepared as described previously, based on known reaction schemes and rate constants for spontaneous aquation/anation.[16,17] Other platinum complexes were prepared in situ directly in the solutions used for the kinetics as described below for each reaction. Stock solutions of mercury(II) perchlorate (0.3 M) were obtained by dissolution of solid HgO (Riedel-de Haen) in 1.0 M perchloric acid. All solutions had an ionic strength of 1.00 M, reached by addition of perchloric acid (Baker's AR) and sodium perchlorate (Baker's AR, recrystallized).

Apparatus. UV/vis spectra were recorded using a Beckman 25 double-beam UV spectrophotometer. Luminescence spectra were obtained with a steady-state Spex Fluorolog spectrofluorometer. A continuous-flow unit with a thermostated flow cell (Hellma QS-178, 2 cm) and a dead time of about 20 ms or the Applied Photophysics scanning facility was used to record the spectra of the short-lived platinum−mercury adducts. Reactions with $t_{1/2}$ > 10 min were monitored using a Zeiss PMQ II spectrophotometer or the Beckman instrument equipped with a thermostated autosampler which protects the solutions from light between the absorbance readings. Reactions with $t_{1/2}$ < ca. 5 s were monitored using a modified Durrum-Gibson stopped-flow instrument or an Applied Photophysics Sequential SX-18 MV stopped-flow instrument. ^{195}Pt NMR spectra were recorded with a Varian Unity 300 spectrometer working at 64.27 MHz. Platinum chemical shifts are reported in parts per million relative to $PtCl_6^{2-}$ ($\delta = 0$) with a solution of $PtCl_4^{2-}$ ($\delta = -1639$ ppm) as the external reference.

Table 1. Experimental Conditions for Kinetics[a]

reaction	λ/nm	C_{Pt}/mM	C_{Cl}/C_{Hg}	C_{Hg}/mM
1	265, 340	0.005, 0.05	0, 1.8[b]	0.05−5
2	320	0.05	0	0.25−25
3	307	0.25	0, 1.0[c]	3.12−100
4	265	0.023	0, 1.0[c]	10−105
5	295	0.175	0	15−100
6	250−275	0.10	0.10[d], 1.0[c]	2.5−100
7	255, 280	0.20	0, 0.5[e]	2−50
8	275	0.25	0	10−50
9	230	0.025	0, 1.0[c]	1−10
10	400	0.5	0, 1.0[c]	2−100
11	400	0.5	0	2.5−100

[a] Complete data in Supporting Information Table S1. [b] Corresponding to 1.9% Hg^{2+}, 16% $HgCl^+$, and 82% $HgCl_2$. [c] Corresponding to 30% Hg^{2+}, 39% $HgCl^+$, and 30% $HgCl_2$. [d] Corresponding to 91% Hg^{2+}, 9% $HgCl^+$, and 30% $HgCl_2$. [e] Corresponding to 60% Hg^{2+}, 31% $HgCl^+$, and 9% $HgCl_2$.

Kinetics. The reactions denoted with numbers 1−11 in Table 2 were initiated by mixing equal volumes of two solutions S and M directly in the stopped-flow instruments or by use of thermostated syringes in spectrophotometer cells. The S solutions contained the substrate platinum complex and sometimes extra chloride. The M solutions contained mercury(II) perchlorate and sometimes extra chloride to assess the effect of $HgCl^+$ and $HgCl_2$. All experiments were performed in an aqueous 1.00 M H^+ (ClO_4^-, Cl^-) medium to prevent protolysis of the platinum(II) and mercury(II) aqua complexes. Since light exposure accelerates these reactions, solutions used for slow kinetics were protected from light except for the short intervals of time needed for reading the absorbance. For total concentrations $C_{Hg} > 10C_{Pt}$, all reactions were first-order with respect to platinum complex. Pseudo-first-order rate constants were calculated from absorbance or transmittance vs time curves using least-squares programs. The experimental conditions are summarized in Table 1, and all kinetics results are given in Supporting Information Table S1. The distributions of mercury between the complexes Hg^{2+}, $HgCl^+$, and $HgCl_2$ as calculated from literature data for the experimental conditions used are given in the footnote to Table 1. Representative plots of k_{obsd} are given in Figure 1 for reactions 10 and 11 (complexes **10** and **11**) and in Supporting Information Figures S1−S9 for all other complexes.

Reaction 1. The reaction was followed by the stopped-flow technique at 265 and 340 nm, where $[HgPtCl_4]$ has absorption maxima with molar absorptivities about 7000 and 800 cm^{-1} M^{-1}, respectively, cf. Figure 2. The S solution was freshly prepared $[PtCl_4]^{2-}$, 5 or 50μM respectively, after mixing. For the Hg(II) concentrations used (Table 1) single exponentials were observed at each wavelength. The subsequent hydrolysis reaction 2 is only a little slower than reaction 1, but for the experimental conditions used, the absorbance change for reaction 2 is negligible, so reaction 1 can be followed without disturbance from 2. Spectra of the accumulated transient product were consistent with that of *cis*-$[PtCl_2(H_2O)_2]$. For C_{Hg} > ca. 5 mM, the spectrum changed due to formation of the adduct, *cis*-$[HgPtCl_2(H_2O)_2]^{2+}$.

Reaction 2. The S solution was $[PtCl_3(H_2O)]^-$ prepared as described previously.[16] The reaction was monitored using the stopped-flow technique at 320 nm. The spectrum of the accumulated product was identical to the final spectrum of reaction 1.

Reaction 3. The S solution contained $[PtCl_4]^{2-}$, which reacts to *cis*-$[PtCl_2(H_2O)_2]$ and *cis*-$[HgPtCl_2(H_2O)_2]^{2+}$ within a few seconds after mixing with mercury(II), reactions 1 and 2. The overall reaction to $[Pt(H_2O)_4]^{2+}$ proceeds via $[PtCl(H_2O)_3]^+$ in the two much slower consecutive reactions 3 and 5. Reaction 3 was followed using ordinary

(10) Venediktov, A. B.; Belyaev, A. V. *Izv. Sib. Otd. Akad. Nauk SSSR, Ser. Khim. Nauk* **1974**, 158.
(11) Pyykkö, P. *Chem. Rev.* **1997**, *97*, 597.
(12) Maliarik, M.; Berg, K.; Glaser, J.; Sandström, M.; Toth, I. *Inorg. Chem.* **1998**, *37*, 2910.
(13) Nagle, J. K.; Balch, L. A.; Ohlmstedt, M. M. *J. Am. Chem. Soc.* **1988**, *110*, 319.
(14) Krumm, M.; Zangrando, E.; Randaccio, L.; Menzer, S.; Danzmann, A.; Holthenrich, D.; Lippert, B. *Inorg. Chem.* **1993**, *32*, 2183.
(15) Balch, A. L.; Fung, E. Y.; Nagle, J. K.; Ohlmstead, M. M.; Rowley, S. P. *Inorg. Chem.* **1993**, *32*, 3295.
(16) Elding, L. I.; Gröning, A. B. *Inorg. Chim. Acta* **1978**, *31*, 243.
(17) Elding, L. I.; Gröning, Ö. *Inorg. Chem.* **1978**, *17*, 1872.

Table 2. Stability Constants K_{Hg} and Kinetic Parameters Determined at 298 K in 1.0 M $HClO_4$ Medium for Hg^{2+}- and $HgCl^+$-Assisted Aquations of Square-Planar Platinum(II) Substrates

reaction	K_{Hg}/M^{-1}	$k_{Hg}/M^{-1}\,s^{-1}$	$k_{HgCl}/M^{-1}\,s^{-1}$	k_{lim}/s^{-1}	k_{aq}/s^{-1} [c]
1. $[PtCl_4]^{2-} \rightarrow [PtCl_3(H_2O)]^-$	$(2.1 \pm 0.4) \times 10^4$	$(2.6 \pm 0.4) \times 10^3$	$(1.05 \pm 0.04) \times 10^3$	0.12	8×10^{-5}
2. $[PtCl_3(H_2O)]^- \rightarrow$ *cis*-$[PtCl_2(H_2O)_2]$	$(8.0 \pm 1) \times 10^2$	$(1.65 \pm 0.8) \times 10^2$		0.20	6×10^{-5}
3. *cis*-$[PtCl_2(H_2O)_2] \rightarrow [PtCl(H_2O)_3]^+$	94 ± 6	$(1.3 \pm 0.1) \times 10^{-1}$	$(7.0 \pm 1) \times 10^{-1}$	1.3×10^{-3}	2×10^{-7}
4. *trans*-$[PtCl_2(H_2O)_2] \rightarrow [PtCl(H_2O)_3]^+$	13 ± 2	13.7 ± 0.9	9 ± 0.8	1.1	1.1×10^{-4}
5. $[PtCl(H_2O)_3]^+ \rightarrow [Pt(H_2O)_4]^{2+}$	5 ± 2	$(5.9 \pm 0.5) \times 10^{-3}$		1.1×10^{-3}	2.8×10^{-7}
6. $[PtCl_3Me_2SO]^- \rightarrow$ *trans*-$[PtCl_2(H_2O)Me_2SO]$	60 ± 6	$(3.6 \pm 0.2) \times 10^4$	$(2.6 \pm 0.04) \times 10^4$	600	9.8×10^{-2}
7. *trans*-$[PtCl_2(H_2O)Me_2SO] \rightarrow$ *cis*-$[PtCl(H_2O)_2Me_2SO]^+$	[b]	3.2 ± 0.2	4.3 ± 0.4	[b]	9.2×10^{-4}
8. *cis*-$[PtCl(H_2O)_2Me_2SO]^+ \rightarrow [Pt(H_2O)_3Me_2SO]^{2+}$	[b]	$(5.7 \pm 0.1) \times 10^{-4}$		[b]	1.4×10^{-6}
9. *trans*-$[PtCl(H_2O)_2Me_2SO]^+ \rightarrow [Pt(H_2O)_3Me_2SO]^{2+}$	[b]	$(9.9 \pm 0.6) \times 10^2$	$(1.3 \pm 0.2) \times 10^3$	[b]	0.5
10. *trans*-$[PtCl_2(NH_3)_2] \rightarrow$ *trans*-$[PtCl(H_2O)(NH_3)_2]^+$	$(3.87 \pm 0.02) \times 10^2$	20.4 ± 0.4	9.4 ± 0.2	0.053	9.8×10^{-5}
11. *cis*-$[PtCl_2(NH_3)_2] \rightarrow$ *cis*-$[PtCl(H_2O)(NH_3)_2]^+$	$(1.90 \pm 0.03) \times 10^2$	20 ± 2		0.104	2.5×10^{-5}
12. $[PtCl(glycine)(NH_3)] \rightarrow [Pt(glycine)(H_2O)(NH_3)]^+$	37[a]	2.1×10^{-2} [a]		5.7×10^{-4} [a]	3.6×10^{-7} [a]

[a] Data from refs 4 and 29. [b] Plots of k_{obsd} vs C_{Hg} strictly linear for $C_{Hg} \leq 50$ mol dm^{-3}. [c] Data from refs 17, 25, 26, and 30.

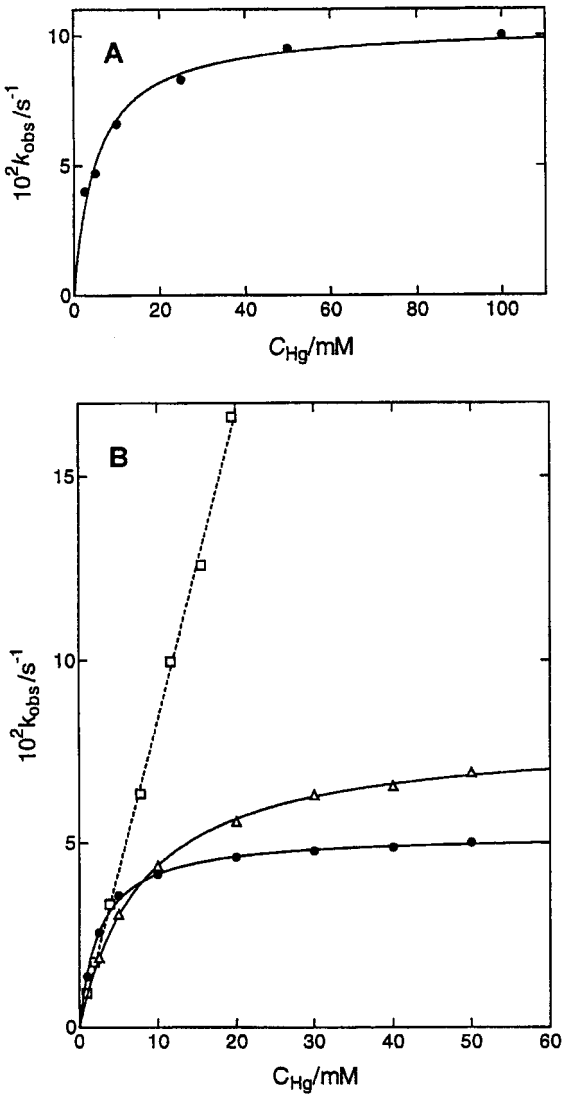

Figure 1. Plots of k_{obsd} vs C_{Hg} for the mercury-assisted aquation for reactions 10 and 11. A: *cis*-$[PtCl_2(NH)_3]$. B: *trans*-$[PtCl_2(NH_3)_2]$. The solid curves represent the fitted eq 5. The distribution of mercury complexes is as follows: (●) 100% Hg^{2+}; (△) 30% Hg^{2+}, 39% $HgCl^+$, and 30% $HgCl_2$; (□) calculated for 100% $HgCl^+$ according to *x*-value = $\alpha_1 C_{Hg}$, *y*-value = $k_{obsd}(1 + K_{Hg}\alpha_o C_{Hg}) - k_{Hg}\alpha_o C_{Hg}$.

spectrophotometry at 307 nm. For mercury(II) concentrations higher than 0.1 M, reactions 3 and 5 are relatively close in rate and therefore difficult to separate, but for the conditions defined in Table 1, reaction 3 is always 5−10 times faster and gives a much larger absorbance change, so it can easily be separated from the subsequent step, cf. Table S1.

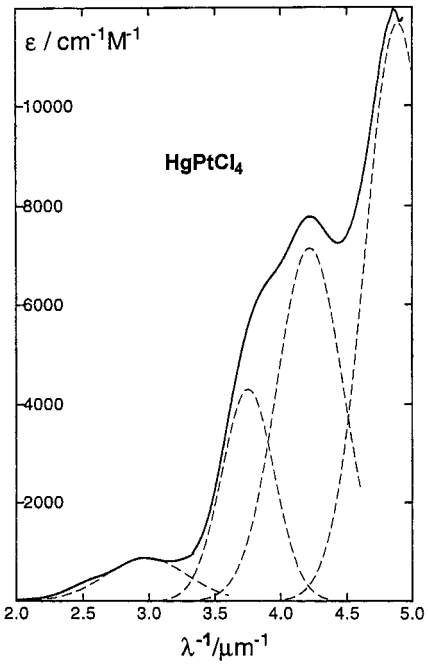

Figure 2. Electronic absorption spectrum of $[HgPtCl_4]$. The dashed lines indicate resolved Gaussian bands in a least-squares analysis.

Reactions 4 and 5. The S solution was *trans*-$[PtCl_2(H_2O)_2]$ prepared as described previously.[16] It was reacted with Hg^{2+} ion in the stopped-flow reactor and monitored at 265 nm. The fast reaction 4 was followed by a much slower process identified as reaction 5, which was monitored using ordinary spectrophotometry at 295 nm. The spectrum of the final product was in good agreement with that of $[Pt(H_2O)_4]^{2+}$.[3]

Reactions 6−8. The S solution was an equilibrated solution of $[PtCl_3Me_2SO]^-$ and *trans*-$[PtCl(H_2O)_2Me_2SO]^+$.[17] In order to study reaction 6, extra chloride was added to the platinum solution before starting the kinetics to restore it to $[PtCl_3Me_2SO]^-$.[17] The very rapid mercury(II)-induced aquation of this complex was then followed by the stopped-flow technique at wavelengths between 250 and 275 nm. Reactions 7 and 8 appeared as subsequent processes that occurred on different time scales. Reaction 7 was followed using ordinary spectrophotometry and a 5 cm cell at 255 or 280 nm, and reaction 8 at 275 nm.

Reaction 9. *trans*-$[PtCl(H_2O)_2Me_2SO]^+$ was obtained by mixing equal volumes of 0.10 mM $[Pt(H_2O)_3Me_2SO]^{2+}$ and 0.35 mM hydrochloric acid. This solution was used for the kinetic runs within 5 min of preparation. Little or no higher chloride complexes are formed within that time.[17] With total concentrations $C_{Pt} = 0.05$ mM and $C_{Cl} = 0.175$ mM the S solution contained an equilibrium mixture of $[Pt(H_2O)_3Me_2SO]^{2+}$ and *trans*-$[PtCl(H_2O)_2Me_2SO]^+$ (60%), cf. equilibrium constants reported previously.[17] Reaction 9 was followed using stopped-flow spectrophotometry at 230 nm.

Table 3. Rate Constants for Chloride Transfer from $HgCl^+$ (k_{-Hg}) to Pt(II) Aqua Complexes and $HgCl_2$ (k_{-HgCl}) and for Their Chloride Anation Reactions (k_{-aq})[a]

trans ligand	Pt(II) substrate and product complex	$k_{-Hg}/M^{-1}\,s^{-1}$	$k_{-HgCl}/M^{-1}\,s^{-1}$	$k_{-aq}/M^{-1}\,s^{-1}$	k_{-aq}/k_{-Hg}
Me_2SO	*trans*-$[PtCl_2(H_2O)Me_2SO] \rightarrow [PtCl_3Me_2SO]^-$	1.6	1.9	18.2[b]	10
	$[Pt(H_2O)_3Me_2SO]^{2+} \rightarrow$ *trans*-$[PtCl(H_2O)_2Me_2SO]^+$	1.3	2.8	3.89×10^3 [b]	3000
Cl^-	$[PtCl_3(H_2O)]^- \rightarrow [PtCl_4]^{2-}$	1.9×10^{-2}	1.4×10^{-2}	5.2×10^{-3} [d]	0.3
	cis-$[PtCl_2(H_2O)_2] \rightarrow [PtCl_3(H_2O)]^-$	1.5×10^{-2}		8.3×10^{-3} [d]	0.9
	$[PtCl(H_2O)_3]^+ \rightarrow$ *trans*-$[PtCl_2(H_2O)_2]$	3.0×10^{-2}	3.0×10^{-2}	0.5[d]	20
	trans-$[PtCl(H_2O)(NH_3)_2]^+ \rightarrow$ *trans*-$[PtCl_2(NH_3)_2]$	1.3×10^{-2}	1.0×10^{-2}	0.31[e]	24
	cis-$[PtCl(H_2O)_2Me_2SO]^+ \rightarrow$ *trans*-$[PtCl_2(H_2O)Me_2SO]$	3.0×10^{-2}	7.1×10^{-2}	20.5[b]	300
NH_3	*cis*-$[PtCl(H_2O)(NH_3)_2]^+ \rightarrow$ *cis*-$[PtCl_2(NH_3)_2]$	1.3×10^{-3}		7.6×10^{-3} [e]	5.8
Gly-O	$Pt(glycine)(H_2O)(NH_3)]^+ \rightarrow [PtCl(glycine)(NH_3)]$	2.6×10^{-5} [c]		1.8×10^{-3} [c]	69
H_2O	$[PtCl(H_2O)_3]^+ \rightarrow$ *cis*-$[PtCl_2(H_2O)_2]$	2.3×10^{-5}	1.3×10^{-5}	2×10^{-3} [d]	90
	$[Pt(H_2O)_4]^{2+} \rightarrow [PtCl(H_2O)_3]^+$	6.5×10^{-5}		2.66×10^{-2} [d]	400
	$[Pt(H_2O)_3Me_2SO]^{2+} \rightarrow$ *cis*-$[PtCl(H_2O)_2Me_2SO]^+$	5.5×10^{-5}		1.4[b]	2500

[a] k_{-Hg}, k_{-HgCl}, and k_{-aq} denote rate constants for the reaction with $HgCl^+$, $HgCl_2$, and Cl^-, respectively. [b] Reference 17. [c] References 4 and 29. [d] References 26 and 30 and references therein. [e] Reference 25.

Reaction 10. The S solution contained 1.0 mM *trans*-$[PtCl_2(NH_3)_2]$ and 1.0 mM added chloride to prevent net hydrolysis, and the reaction was followed by the stopped-flow technique at 400 nm.

Reaction 11. The S solution of 1.0 mM *cis*-$[PtCl_2(NH_3)_2]$ in 1.0 M $HClO_4$ was freshly prepared for each batch of kinetics and mixed within 1 h in the stopped-flow device with M solutions containing various concentrations of Hg^{2+}. The kinetics for *cis*-$[PtCl_2(NH_3)_2]$ reacting with Hg^{2+} follows the same pattern as that for the trans isomer. The rate processes for the removal of the first and second chloride ions were separated by use of the Applied Photophysics kinetics program. The rate constants for the second reaction were consistently less than those for the first one (>30- to 4-fold) over the range of increasing Hg^{2+} concentrations used.

Product Analysis by ^{195}Pt NMR. Some reactions were also followed by ^{195}Pt NMR spectroscopy primarily to verify the sequential reactions and their stereochemistry and to identify intermediates and final reaction products.

Computational Details. All DFT calculations employed the Amsterdam Density Functional program package version 1999.02.[18,19] All geometries were optimized using ADF basis sets IV (triple-ζ STO plus polarization) with frozen cores (up to 4f on Pt and Hg, 2p on Cl, and 1s on O) at the scalar relativistically corrected[20,21] Local Density Approximation[22] level with the Vosko−Wilk−Nusair correlation functional.[23] Default convergence criteria were applied throughout.

Results

UV/Vis Kinetics. Aquations in the presence of mercury are much faster than the spontaneous ones (k_{aq}). The rates depend on the concentrations of Hg^{2+} as well as $HgCl^+$. In complexes with more than one chloride bound to platinum, the chlorides are removed in sequential reactions with separable rate constants. These sequential processes were also verified by NMR (vide infra). The results can be described by the stoichiometric reactions of eqs 1−3, which also define the equilibrium and rate constants used.

$$PtL_3Cl + Hg^{2+} \underset{\text{fast}}{\overset{K_{Hg}}{\rightleftharpoons}} [Pt,Hg^{2+}\ \text{adduct}] \quad (1)$$

$$PtL_3Cl + Hg^{2+} \underset{k_{-Hg}}{\overset{k_{Hg}}{\rightleftharpoons}} PtL_3OH_2 + HgCl^+ \quad (2)$$

$$PtL_3Cl + HgCl^+ \underset{k_{-HgCl}}{\overset{k_{HgCl}}{\rightleftharpoons}} PtL_3OH_2 + HgCl_2 \quad (3)$$

Spectra. The rapid associations between Hg^{2+} ion and the platinum(II) complexes were observed qualitatively by instantaneous color and intensity changes on mixing which were observed visually as well as spectrophotometrically. Mixing of concentrated solutions of red $[PtCl_4]^{2-}$ and transparent Hg^{2+} ion gave a bright yellow precipitate that darkened during drying. The overall mercury-assisted reaction from $[PtCl_4]^{2-}$ to $[Pt(H_2O)_4]^{2+}$ is strongly accelerated by visible light, and illumination of solutions containing $[HgPtCl_4]$ at 250 nm initiates luminescence at 565 nm. All these observations are compatible with metal−metal interactions.[11]

The accessible spectral range for quantitative investigations of the platinum−mercury adducts was determined by the concentration of free Hg^{2+} needed for the adduct to accumulate. The stability constants determined from the kinetics (eq 4 below) are given in Table 2. For $[HgPtCl_4]$ an almost complete (95%) accumulation required a free Hg^{2+} ion concentration of only 1 mM, and the spectrum was reliably recorded down to 210 nm. The other adducts could only be investigated in a more limited spectral range due to higher background absorbance. Examples of the absorption spectra are displayed in Figures 2, 3, and S11. Individual absorbance bands were resolved from the spectral data by least-squares fittings of ϵ vs $1/\lambda$ Gaussian band shapes. Spectral assignments are given in Table 4. The charge transfer bands were assigned to transitions from platinum 5d to mixtures of mainly Hg 6s and Pt 6p orbitals. The alternative LMCT origin Pt ← Cl influenced by Hg^{2+} is less likely since these transitions are known to show a large blue shift when chloride ligands are replaced by ammonia or oxygen.[24] The band positions observed, $3.75 \approx 3.75 < 3.2\ \mu m^{-1}$ for $[HgPtCl_4]$, $[HgPtCl_3(H_2O)]^{2+}$, and $[HgPt(glycine)(NH_3)Cl]^{2+}$,[10] respectively, are the inverse of those expected for transitions of the LMCT type. The origin of the CT bands is the same in the different complexes as indicated by their nearly equal intensity and the large red shift as compared to any CT bands in the corresponding substrate complexes. The relatively broad band at $2.9\ \mu m^{-1}$ of $[HgPtCl_4]$ is assigned to a ligand field transition in spite of its relatively large intensity ($\epsilon = 870\ cm^{-1}\ M^{-1}$). This band can be traced from $[HgPtCl_4]$

(18) Baerends, E. J.; Bérces, A.; Bo, C.; Boerrigter, P. M.; Cavallo, L.; Deng, L.; Dickson, R. M.; Ellis, D. E.; Fan, L.; Fischer, T. H.; Fonseca Guerra, C.; van Gisbergen, S. J. A.; Groeneveld, J. A.; Gritsenko, O. V.; Harris, F. E.; van den Hoek, P.; Jacobsen, H.; van Kessel, G.; Kootstra, F.; van Lenthe, E.; Osinga, V. P.; Philipsen, P. H. T.; Post, D.; Pye, C. C.; Ravenek, W.; Ros, P.; Schipper, P. R. T.; Schreckenbach, G.; Snijders, J. G.; Sola, M.; Swerhone, D.; te Velde, G.; Vernooijs, P.; Versluis, L.; Visser, O.; van Wezenbeek, E.; Wiesenekker, G.; Wolff, S. K.; Woo, T. K.; Ziegler, T. *ADF 1999.02*; Scientific Computing and Modelling NV, Free University: Amsterdam, 1999.
(19) Fonseca Guerra, C.; Snijders, J. G.; te Velde, G.; Baerends, E. J. *Theor. Chem. Acc.* **1998**, *99*, 391.
(20) Snijders, J. G.; Baerends, E. J.; Ros, P. *Mol. Phys.* **1979**, *38*, 1909.
(21) van Lenthe, E.; Snijders, J. G.; Baerends, E. J. *J. Chem. Phys.* **1993**, *99*, 4597.
(22) Slater, J. C. *Adv. Quantum Chem.* **1972**, *6*, 1.
(23) Vosko, S. H.; Wilk, L.; Nusair, M. *Can. J. Phys.* **1980**, *58*, 1200.
(24) Elding, L. I.; Olsson, L. F. *J. Phys. Chem.* **1978**, *82*, 69.

Table 4. Wave Numbers (in μm^{-1}) and Molar Absorptivities (within Parentheses, in M^{-1} cm^{-1}) with Proposed Assignments for Platinum−Mercury Adducts (Aqua Ligands Excluded)

$[HgPtCl_4]$	$[HgPtCl_3]^+$	*cis*-$[HgPtCl_2]^{2+}$	$[HgPtCl(gly)(NH_3)]^+$	$[PtCl_4]^{2-}$	assgnmnt for $[PtCl_4]^{2-}$ [d]	excited state D_{4h} [e]	assgnmnt for $[HgPtCl_4]$ [d,g]	excited state [g]
2.27 (40)	2.4 (49)	2.20 (16)		2.10 (17)[c]	$b_{1g} \leftarrow e_g$	$^3B_{1g}$	–	–
2.49 (120)	2.58 (150)	2.84 (76)		2.56 (56)[c]	$b_{1g} \leftarrow b_{2g}$	$^1A_{2g}$	$b_1 \leftarrow b_2$	$^1A_2$
2.99 (870)	3.08 (780)	3.25 (283)		3.02 (59)[c]	$b_{1g} \leftarrow e_g$	^1E_g	$b_1 \leftarrow e$	^1E
3.75 (4300)	3.75 (4000)	4.03 (1517)	3.44 (3800)[b]	4.34 (7200)[c]	$2a_{2u} \leftarrow b_{2g}$	^3E_g[f]	$2a_1 \leftarrow b_2$	^3E[f]
4.22 (7140)	–[a]	–	3.84 (7800)[b]	4.65 (9050)[c]	$2a_{2u} \leftarrow e_g$	^3E_g, $^3A_{2u}$	$2a_1 \leftarrow e$	^3E, $^3A_1$
4.89 (11700)	–	–	–				–	

[a] A dash denotes not observable due to high background absorbance from mercury. [b] From spectrum in reference 10. [c] Data from reference 24. [d] Assignments see Figure 5. [e] States which can be reached via electric dipole allowed transitions have symmetry E_u or A_{2u} in D_{4h}. These states correlate to E and A_1 respectively, in C_{4v} symmetry. [f] The singlet states B_{1u} and A_2 for D_{4h} and C_{4v} respectively are symmetry forbidden but the corresponding singlet−triplet transition is allowed via spin−orbit coupling. [g] Assuming axial addition of Hg^{2+} giving local C_{4v} symmetry around platinum.

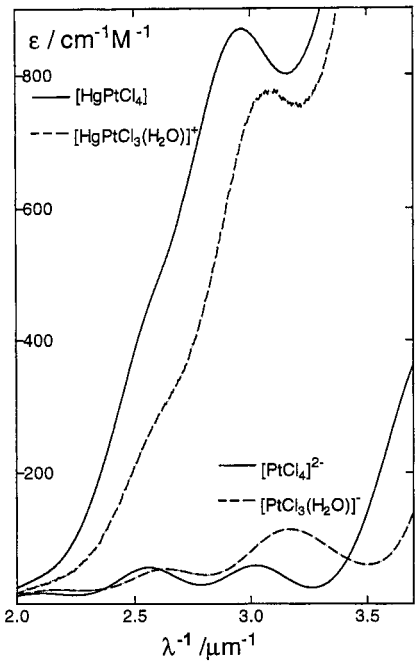

Figure 3. Visible absorption spectra of $[HgPtCl_4]$ and $[HgPtCl_3(H_2O)]^+$ together with the spectra of the parent platinum complexes.

via $[HgPtCl_3(H_2O)]^+$ to *cis*-$[HgPtCl_2(H_2O)_2]^{2+}$, and as can be seen from Figure 3 and Table 4, the band is tied to the position of the ligand field transition $b_{1g} \leftarrow e_g$ in the parent platinum(II) substrates. Also, it is not evident in the published spectrum of $[HgPt(glycine)(NH_3)Cl]^{2+}$,[10] where the higher ligand field strength in this complex probably moves the band under the first CT band which appears at 3.2 μm^{-1} (Supporting Information Figure S11). The ^1E_g state derived from this transition can split considerably in lower ligand field symmetries. However, attempts to resolve the broad band into two bands of similar intensity did not improve the overall least-squares fit. The weak shoulder at the visible side of the band corresponding to a resolved band at 2.49 μm^{-1} in $[HgPtCl_4]$ is connected to the transition $b_{1g} \leftarrow e_g$ on the same grounds as the first band assignment. One additional observed band at still lower energies is connected to singlet−triplet ligand field transitions.

Effect of Hg^{2+}. The observed rate constants for the Hg^{2+}-assisted aquations could be reproduced by use of eq 4 for all the substrates. The three sulfoxide complexes **7**−**9** gave strictly linear plots with large second-order rate constants k_{Hg} and small intercepts identified as the spontaneous aquation rate constant k_{aq}, i.e., $K_{Hg} = 0$ for **7**−**9**. The aquation rate constants k_{aq} given in Table 2 have been published previously for all the investigated substrates.[17,25,26,30] They were used as fixed parameters in the

$$k_{obsd} = \frac{k_{aq} + k_{Hg}[Hg^{2+}]}{1 + K_{Hg}[Hg^{2+}]} \quad (4)$$

curve fittings to determine the values of k_{Hg} and K_{Hg} given in Table 2 together with the limiting values $k_{lim} = k_{Hg}/K_{Hg}$. There is a good linear correlation between log k_{lim} and log k_{aq} reflecting the variation in the trans effect for the donor atoms O < Cl, N < S (Supporting Information Figure S10). The linear regression line has a correlation coefficient of 0.96 and a slope of 1.02 ± 0.08. This implies that the ratio between k_{lim} and k_{aq} is nearly constant over a range of 6 orders of magnitude. The intercept of the line is 3.6 ± 0.4, i.e., the limiting values for the Hg^{2+}-assisted aquations are on average ca. 4000 times faster than the spontaneous ones.

Effect of $HgCl^+$. The effect of $HgCl^+$ was studied using mercury(II) solutions with mean chloride ligand numbers calculated as C_{Cl}/C_{Hg} in the range 0−1.8. Under these conditions, only the aquated mercury complexes Hg^{2+}, $HgCl^+$, and $HgCl_2$ are present in appreciable concentrations. Their mole fractions α_n (n = 0, 1, 2) were calculated from the stability constants in the literature (footnote, Table 1).[27] The α_n values were held constant as the total mercury(II) concentration was varied. An independent experiment with pure $HgCl_2$ showed that its contribution was negligible compared to those of $HgCl^+$ or Hg^{2+}.[28] The combined accelerating effect of these two complexes could be described with the parametric equation 5, where k_α and K_α are conditional constants determined by least-squares fitting. The individual contributions from $HgCl^+$ and

$$k_{obsd} = \frac{k_{aq} + k_{Hg}[Hg^{2+}] + k_{HgCl}[HgCl^+]}{1 + K_{Hg}[Hg^{2+}] + K_{HgCl}[HgCl^+]} = \frac{k_{aq} + (k_{Hg}\alpha_0 + k_{HgCl}\alpha_1)C_{Hg}}{1 + (K_{Hg}\alpha_0 + K_{HgCl}\alpha_1)C_{Hg}} \equiv \frac{k_{aq} + k_\alpha C_{Hg}}{1 + K_\alpha C_{Hg}} \quad (5)$$

Hg^{2+} to the conditional constants were resolved using α_0 and α_1 from Table 1. The contribution to k_α from these two ions gave roughly equal second-order rate constants for $HgCl^+$ and Hg^{2+} activation in each instance. However, within the experimental errors, no contribution to K_α from $HgCl^+$ was detected,

(25) Tucker, M. A.; Colvin, C. B.; Martin, D. S. *Inorg. Chem.* **1964**, *3*, 1373.
(26) Elding, L. I. *Inorg. Chim. Acta* **1978**, *28*, 255.
(27) Ciavatta, L.; Grimaldi, M. *J. Inorg. Nucl. Chem.* **1968**, *30*, 197.
(28) The hydrolysis of 1 mM $PtCl_4^{2-}$ in a solution of 20 mM $HgCl_2$ containing 5 mM NaCl to suppress formation of $HgCl^+$ showed that the effect of $HgCl_2$ was negligible.
(29) Venediktov, A. B.; Belyaev, A. V. *Izv. Sib. Otd. Akad. Nauk SSSR , Ser. Khim. Nauk* **1976**, 52.
(30) Elding, L. I. *Acta Chem. Scand.* **1970**, *24*, 1527.

i.e., $K_{HgCl} = 0$. Thus, the saturation in the plots of k_{obsd} vs C_{Hg} can be attributed to Hg^{2+} exclusively. All association and rate constants are given in Table 2.

Plots of k_{obsd} vs C_{Hg} for kinetic experiments with Hg^{2+} ion alone and for experiments with a constant distribution of Hg^{2+}, $HgCl^+$, and $HgCl_2$ are exemplified in Figure 1, using *cis*- and *trans*-$[PtCl_2(NH_3)_2]$ as substrates. A limiting rate was reached for the first aquation process at ca. 0.05 M Hg^{2+}, and the overall data fit a rate law of the form shown in eqs 4 and 5. These results lead to association constants K_{Hg} for Hg^{2+} binding to the cis (**11**) and trans (**10**) isomers of 190 ± 3 and 387 ± 2 M^{-1}, respectively, along with rate constants k_{Hg} of 20 ± 2 and 20.4 ±0.4 M^{-1} s^{-1}, respectively. Clearly the binding constant for the cis isomer is less than that for the trans, which implies that Hg^{2+} is not symmetrically attached to two chloride ligands in the coordination plane of the platinum complex to any significant degree.

Figure 1 also displays a plot of the resolved rate contribution for $HgCl^+$. It shows a strict linear dependence on concentration illustrating that adduct formation between $HgCl^+$ and platinum is negligible. Similar observations are evident for all other substrates with saturation kinetics (Supporting Information Figures S1−S6).

Reverse Reactions. From the values of the second-order rate constants for the mercury-assisted aquations, the second-order rate constants for the reverse processes, eqs 2 and 3, were calculated using eqs 6 and 7 and literature values for the stability

$$k_{-Hg} = k_{Hg}\frac{K_{PtCl}}{K_{HgCl}} \quad (6)$$

$$k_{-HgCl} = k_{HgCl}\frac{K_{PtCl}}{K_{HgCl_2}} \quad (7)$$

constants K_{PtCl} for the platinum substrates.[17,25,26,29] The values are given in Table 3 together with rate constants for the chloride anation processes. A direct observation of the reverse chloride transfer from $HgCl^+/HgCl_2$ to $[PtCl(H_2O)_3]^+$ (reverse reaction 4) was observed by NMR (vide infra).

***cis*- and *trans*-$[Pt(NH_3)_2Cl_2]$ + Hg^{2+} Followed by ^{195}Pt NMR.** At 25 °C, *cis*-$[PtCl_2(NH_3)_2]$, **11**, was rapidly dissolved in a D_2O solution of $Hg(ClO_4)_2$ containing 0.011 M CF_3SO_3H to give final concentrations of Pt and Hg of 20 and 10 mM, respectively. After 5 min a relatively sharp signal ($^1J(^{195}Pt-^{14}N)$ = 254 Hz, $\Delta\nu_{1/2}$ = 100 Hz, quintuplet) at −1830 ppm due to *cis*-$[PtCl(OH_2)(NH_3)_2]^+$ was evident, along with a broad signal ($\Delta\nu_{1/2} \approx 6000$ Hz) without fine structure centered about −2080 ppm. This signal may reflect the presence of the mercury adduct. No sharp signal from *cis*-$[PtCl_2(NH_3)_2]$ at 2155 ppm could be observed. After 2000 s signals at −1590 and −1830 ppm due to the bis aqua and chloro aqua ions, respectively, were the only ones evident. In the presence of excess Hg^{2+}, the signal for the *cis*-diaqua diammine ion was observed rapidly after mixing (−1628 ppm, $^1J(^{195}Pt-^{14}N)$ = 266 Hz, $\Delta\nu_{1/2}$ = 100 Hz, quintuplet).

The trans isomer (**10**) showed similar behavior. Equimolar ratios of Hg^{2+} and *trans*-$[PtCl_2(NH_3)_2]$ (8 mM each in D_2O containing 0.011 M CF_3SO_3H) at 25 °C led first to the *trans*-chloro aqua ion (−1807 ppm) and then to the *trans*-diaqua ion (−1410 ppm). These were the only products observed over 12 h.

$[PtCl_4]^{2-}$ + Hg^{2+} by ^{195}Pt NMR. The reaction between $[PtCl_4]^{2-}$ and Hg^{2+} was also followed by ^{195}Pt NMR spectrometry. For $[PtCl_4]^{2-}$ (40 mM) plus Hg^{2+} (20 mM) at 25 °C in D_2O (0.10 M $HClO_4$), 85 s after mixing, sharp signals (ca. 100 Hz) for the parent ion (−1639 ppm), the initial product, $[PtCl_3(H_2O)]^-$ (−1195 ppm), and *cis*-$[PtCl_2(H_2O)_2]$ (−833 ppm), the subsequent product, appeared. Within ca. 45 min equilibrium was established between the three species in the ratio 1:10:1, and this was essentially maintained for 5 h. After 17 h, a signal for a trace of the *trans*-$[PtCl_2(H_2O)_2]$ isomer also emerged at −647 ppm. For an equimolar Pt:Hg ratio, the parent ion was no longer observed after 96 s and only the trichloroaqua and *cis*-dichlorodiaqua complexes **2** and **3** were evident. However, within 1 h, some *trans*-dichloro diaqua isomer **4** was observed, and this signal continued to increase. Moreover, a Pt:Hg ratio of 2:3 gave significant concentrations of chlorotriaqua $[PtCl(H_2O)_3]^+$ (−378 ppm) (25%) and *trans*-dichlorodiaqua complexes (10%) along with the cis complex (60%) within 1.5 h as the sole observed components in the reaction mixture except for a trace of the trichloroaqua complex (<5%). Over 12 h, the cis−trans equilibrium between **3** and **4** was established as essentially a 1:1 mixture, and the ratio of dichloro:monochloro complexes remained constant, i.e., 3:1, plus a trace (<5%) of the trichloro ion for at least 17 h. These results not only give a direct measurement of the cis−trans equilibrium constant at 25 °C in 1.0 M $HClO_4$ for $[PtCl_2(H_2O)_2]$ as $K_{c/t}$ = 1.02, in good agreement with the literature value for the uncatalyzed process of 1.2 ± 0.1,[30] but also indicate that a $HgCl^+/HgCl_2$ mixture catalyzes the rate of equilibration with a $t_{1/2}$ of ca. 3 h at 25 °C, several orders of magnitude faster than the spontaneous equilibration.[30] Finally, an excess of Hg^{2+} ion (2.5-fold over Pt) led within 0.5 h to $[Pt(H_2O)_4]^{2+}$ (3 ppm) and $[PtCl(H_2O)_3]^+$ (−372 ppm) as the only observed components in the reaction mixture. Ultimately, the tetra-aqua ion dominated the mixture (8:1) and this ratio was constant for at least 12 h. These findings are consistent with the reaction model proposed for the spontaneous stepwise aquations of $[PtCl_4]^{2-}$.[30] The mercury acceleration of both forward and reverse reactions is very efficient, compared to the spontaneous aquation in 0.1 mM $[PtCl_4]^{2-}$, which requires at least 2000 h to reach equilibrium at 25 °C.[30]

Essentially, both sets of investigations show sequential removal of coordinated Cl^- ions from the Pt(II) substrates in contrast to what has been proposed for complex **11** previously.[9] Isomerization of $[PtCl_2(H_2O)_2]$ takes place via aquation/anation processes. Formation of the trans isomer is fast when the system is dominated by $[PtCl(H_2O)_3]^+/HgCl_2$ or *cis*-$[PtCl_2(H_2O)_2]/HgCl_2$, in qualitative agreement with the rate constants for the reverse reactions given in Table 3.

Discussion

Structure and Stability of the Adducts. The absence of a chelate effect for the Hg^{2+} adduct of *cis*-$[PtCl_2(NH_3)_2]$ as compared to the trans isomer strongly indicates that the adducts are not stabilized by chloride bridges. In addition, the trans isomers form stable adducts with Hg^{2+} but not with $HgCl^+$, in spite of the fact that these two Hg species have a similar affinity for chloride.[27] A further argument against halide bridges is the fact that no adducts were observed in the mercury-assisted aquation of axially blocked $[Pd(Et_4dien)X]^+$ (X = halide or SCN^-).[6,8]

Geometry-optimized structures of models for metal−metal adducts of $[PtCl_4]^{2-}$ with $[Hg(H_2O)]^{2+}$ or $[HgCl]^+$ are shown in Figure 4. The position of the mercury is almost axial, indicating that the metal−metal bond is formed without strong assistance from a chloride ligand in the Pt(II) coordination plane. The theoretical structural results appear to be consistent with

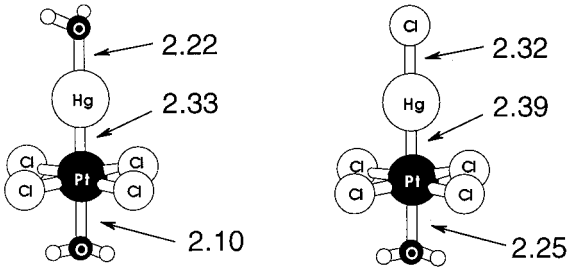

Figure 4. Geometry-optimized structures of hydrated $[HgPtCl_4]$ and $[ClHgPtCl_4]^-$.

the experimental observation of $[HgPtCl_4]$ but not $[ClHgPtCl_4]^-$, inasmuch as the Pt−Hg(OH_2) distance is 0.06 Å shorter than the Pt−HgCl contact. The metal−metal interaction also weakens the Hg−L bond but much more so for L = H_2O. The Hg−O distances in linear $[Hg(H_2O)_2]^{2+}$ are computed to be 2.00 Å while the Hg−Cl bonds in $HgCl_2$ are 2.25 Å long. Relative to the HgL_2 species, then, the Hg−O and Hg−Cl bonds lengthen by over 0.2 and 0.07 Å, respectively, in the relevant adducts. The Pt−OH_2 bond trans to Hg is also noticeably shorter for $[HgPtCl_4]$, prompting the speculation that the Pt center in $[HgPtCl_4]$ has more Pt(IV) character, and hence greater kinetic and thermodynamic stability, than $[ClHgPtCl_4]^-$. If the trans aqua ligand of Pt(II) is excluded, giving a square-pyramidal rather than an octahedral geometry, the Cl−Pt−Hg angle decreases to 80°, reflecting a greater bridge assistance.

For the $[PtCl_n(H_2O)_{4-n}]^{2-n}$ (n = 1−4) complexes, the magnitude of K_{Hg} decreases approximately 1 order of magnitude for each aqua ligand introduced (Table 2). In addition to electrostatic contributions, the decreasing covalent interactions between Hg^{2+} and the platinum complexes due to contraction of the Pt d-orbitals through the series of complexes when chloride is exchanged for water is probably important for this trend. The effect is expected to be large for the heavier transition metals due to the relativistic contraction of the valence s-orbitals and the penetration into the d-shell. The observation that the K_{Hg} values for the Me_2SO complexes are smaller than those for analogous aqua or ammine complexes is also consistent with a stabilization of the metal d-orbitals due to the greater π-acid strength of the S-bonded sulfoxide ligand.[31]

UV/Vis Spectra of the Adducts. The qualitative effects on the electronic structure due to axial interactions between the Pt(II) substrates and the Hg^{2+} ion can be inferred from empirical and theoretical results on related systems.[13,32−36] A partial MO diagram showing these effects for the $[PtCl_4]^{2-}$−Hg^{2+} system is displayed in Figure 5. A new orbital (which is mainly Hg 6s) appears at lower energy than the original a_{2u} orbital, which is mainly platinum $6p_z$. The arrows indicate the transitions connected with the observed bands, cf. Table 4.

In aqueous solution, the $[PtCl_4]^{2-}$ complex displays only two high-intensity bands at 4.65 and 4.34 μm^{-1}. From MCD measurements the first band has been assigned to the transition $a_{2u} \leftarrow e_g$.[37] There seems to be no disagreement in the literature concerning the d−p origin of this band.[38] Spectral data for the

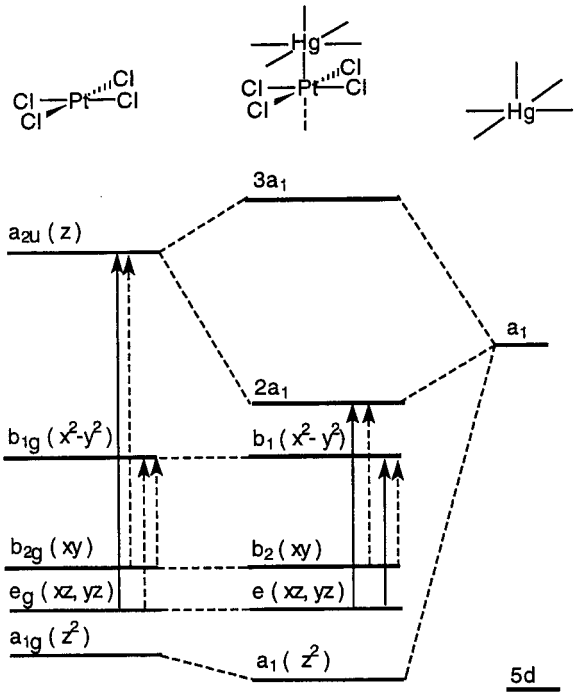

Figure 5. Partial one-electron MO diagram for $[PtCl_4]^{2-}$ and $[HgPtCl_4]$ (including solvent water) showing the proposed assignments for the latter and the correlation to the more well-established bands of $[PtCl_4]^{2-}$. A dashed arrow indicates that the spin-allowed interconnection is electric dipole forbidden in the local symmetry of D_{4h} or C_{4v}.

other band can be reconciled both with a triplet state of the $a_{2u} \leftarrow b_{2g}$ transition and with an LMCT origin.[37] More recently, however, both bands were ascribed to internal singlet−triplet d−p transitions.[38] On the assumption of a square-pyramidal structure of $[HgPtCl_4]$, the bands with MLCT characteristics occurring at 4.2 and 3.75 μm^{-1} can therefore naturally be connected with the proposed d−p transitions in $[PtCl_4]^{2-}$. The assignments of the CT bands given in Table 4 are analogous to those made for solid $Tl_2[Pt(CN)_4]$.[13,33] The assignments of the individual bands, however, for the complexes studied here have been adopted to fit the relative energies of the mainly d-based orbital energies in $[PtCl_4]^{2-}$, $a_{1g} < e_g < b_{2g}$, which occur in a reverse order to those of $[Pt(CN)_4]^{2-}$.[33,39] If the band at 3.75 μm^{-1} is tentatively assigned to an LMCT transition, the large red shift would be consistent with an enhanced charge on the Pt(II) metal center. This could occur for Hg−Pt interactions but hardly for a bridged complex without a parallel effect on the d−d bands, which is not observed.

For the ligand field transitions, the large intensity enhancement of the $b_{1g} \leftarrow e_g$ transition in going from $[PtCl_4]^{2-}$ to $[HgPtCl_4]$ ($b_1 \leftarrow b_2$) is of a relative magnitude similar to that observed for one of the singlet−triplet components of this transition in Magnus's green salt (for notations and assignments, see Figure 5 and Table 4).[40] The selective enhancement of this band as compared to the $b_1 \leftarrow b_2$ transition is also dictated by group theory for the C_{4v} symmetry. Given that the ordering of the mainly d-based molecular orbital energies in $[PtCl_4]^{2-}$ $a_{1g} < e_g < b_{2g}$ is the same in $[HgPtCl_4]$, the $b_1 \leftarrow b_2$ transition should lie at the visible side of the more intense $b_1 \leftarrow e$ transition. Accordingly, a weak shoulder is observed.

Mechanism. It is well-known that substitution reactions at Pt(II) substrates similar to those studied here are subject to

(31) Kukushkin, Yu. N.; Spevak, V. N. *Zh. Neorg. Khim.* **1972**, *17*, 1686.
(32) van der Ploeg, A. F. M. J.; van Koten, G.; Schmitz, J. E. J.; van der Linden, J. G. M. *Inorg. Chim. Acta* **1982**, *58*, 53.
(33) Ziegler, T.; Nagle, J. K.; Snijders, J. G.; Baerends, E. J. *J. Am. Chem. Soc.* **1989**, *111*, 5631.
(34) Interrante, L. V.; Bundy, F. P. *Inorg. Chem.* **1971**, *10*, 1974.
(35) Aullón, G.; Alvarez, S. *Inorg. Chem.* **1996**, *35*, 3137.
(36) Dolg, M.; Pyykkö, P.; Runeberg, N. *Inorg. Chem.* **1996**, *35*, 7450.
(37) Isci and, H.; Mason, W. R. *Inorg. Chem.* **1984**, *23*, 1565.
(38) Olsson, L. F. *Inorg. Chem.* **1986**, *25*, 1697.
(39) Vanquickenborne, L. G.; Ceulemans, A. *Inorg. Chem.* **1981**, *20*, 796.
(40) Interrante, L. V.; Bundy, F. P. *Inorg. Chem.* **1971**, *10*, 1169.

Scheme 1. Mechanism A

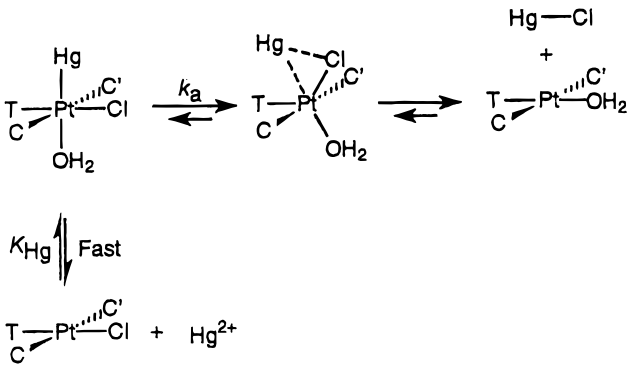

Scheme 2. Mechanism B

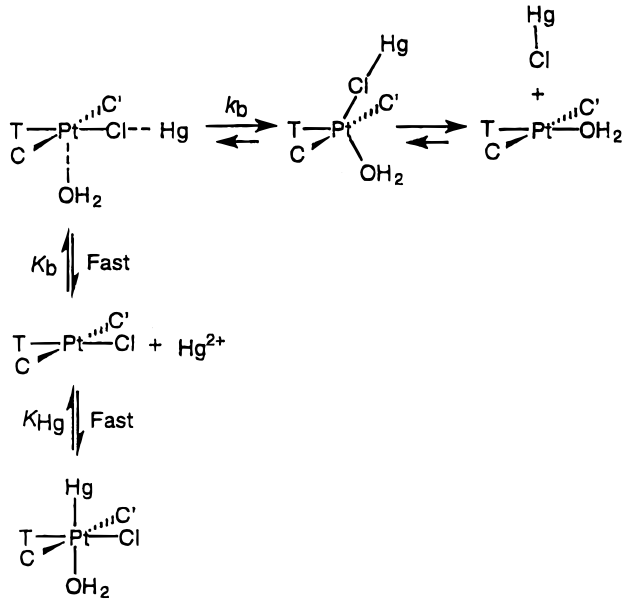

electrophilic catalysis by Lewis acids. For example, chloride exchange at *trans*-[$PtCl_2py_2$] is strongly accelerated by H_3BrO_3,[41] and chloride displacement from *trans*-[$PtCl_2(pip)_2$] is catalyzed by HNO_2.[42] In these systems, electrophilic catalysis is the only possibility, since the catalyst has no affinity for the leaving chloride ligand at platinum. The proposed mechanism involves a rapid addition of the Lewis acid to the axial position of the Pt(II) substrate followed by a facilitated attack by the entering ligand. In the case of HNO_2 catalysis, UV/vis spectra of axial adducts have also been identified.[42] In the present systems, there is a possibility of acceleration via attack by Hg(II) on the leaving chloride ligand, as well as electrophilic catalysis by Hg^{2+}. These two limiting cases are schematically represented in Schemes 1 and 2.

Path A (Scheme 1) involves an accumulated Pt−Hg adduct which decomposes into a Pt(II)−aqua complex and $HgCl^+$. This path is favored by the reduced d-electron density at Pt(II) caused by Hg^{2+}, facilitating the addition of the entering water molecule. In addition, the mercury(II) ion could assist the release of the leaving chloride. On the other hand, both empirical and theoretical results show that axial d^8-d^{10} metal−metal interactions stabilize a flat geometry of the Pt(II) fragment.[33] Hence, the adduct appearing as an intermediate along path A will resist rearrangement into a TBP structure. In other words, the metal−metal bond has to be partly broken in the transition state. In this mechanism, the overall second-order rate constant is $K_{Hg}k_a$.

In path B (Scheme 2) the aquation proceeds via the standard bridge mechanism, and the rapidly equilibrating Pt−Hg adducts observed are not intermediates along the reaction coordinate. A weak chloride-bridged complex forms independently and undergoes aquation by water attack at the Pt(II) center. While the initial binding of the entering water ligand may be weaker in this case since the Pt center is less positively charged, the mercury assists the leaving group. This pathway is limited by the expected low concentration of the reactive single-bridged complex, but it is favored by a transition state effect. The σ-donor strength of the Cl−Hg group is expected to be low, and according to current theories for Pt(II) substitution mechanisms this ligand will therefore readily go into an equatorial site of a trigonal-bipyramidal transition state.[43] The more linear Pt−Cl−Hg arrangement would also be more efficient in releasing the chloride ligand from the metal center. In this mechanism, the Pt−Hg adducts represent a "dead end" in the kinetics scheme.

Experimental observations favor the bridge model B. For example, the values of the rate constants k_{Hg} and k_{HgCl} are practically the same in each instance, in spite of the fact that the electrophilic interactions between platinum and mercury are much stronger for Hg^{2+}, cf. Table 2. This is an indication that the metal−metal interaction is absent in the transition state. Moreover, the rate constants k_{-Hg} for the reverse chloride transfer reactions from $HgCl^+$ to platinum are practically independent of the substrate charge and the nature of the cis ligands (Table 3). This is best rationalized by a linear Pt−Cl−Hg fragment in the transition state. Such a structure reduces the electrostatic interactions, since the entering chloride is only partly transferred to the platinum compared to an ordinary chloride anation, where the charge dependence is strong. The Pt−Hg distance is also long compared to the more compact transition state structure in mechanism A. If mechanism B is operative, the observed rate constant at saturation, k_{lim}, is expressed as $k_bK_b/(K_b + K_{Hg}) \approx k_bK_b/K_{Hg} = k_{Hg}/K_{Hg}$, where the factor K_b/K_{Hg} represents the retardation due to the formation of the Pt−Hg adducts.

The rate constants for chloride transfer from $HgCl^+$ and $HgCl_2$ to platinum are comparable to the chloride anation rate constants for neutral and anionic substrates (Table 3). The variation in k_{-Hg} and k_{-HgCl} due to the different trans ligands is $1:300:10^5$ for water, chloride, and dimethyl sulfoxide, respectively, which is similar to that reported previously for nucleophilic substitution reactions.[17] Path B also accommodates the retention of configuration where relevant, and the isomerization of *cis*- and *trans*-[$PtCl_2(H_2O)_2$] via consecutive substitutions as outlined in earlier work.[30]

Acknowledgment. Thanks are due to Ms. Bodil Eliasson and Dr. Rosaria Plutino for experimental assistance, to Dr. Ola F. Wendt for valuable comments, to the Swedish Natural Science Research Council and the Royal Physiographic Society of Lund for financial support, and to the Royal Swedish Academy of Sciences and Wenner-Gren Foundation for a visiting professorship to A.M.S.

Supporting Information Available: Observed first-order rate constants for mercury(II)-assisted aquation in 1.00 M $HClO_4$ medium at 25.0 °C (Table S1) and plots of k_{obsd} vs C_{Hg} for the mercury-assisted aquations of $[PtCl_4]^{2-}$, $[PtCl_3(H_2O)]^-$, *cis*-[$PtCl_2(H_2O)_2$], *trans*-[$PtCl_2$-

(41) Pearson, R. G.; Gray, H. B.; Basolo, F. *J. Am. Chem. Soc*. **1960**, *82*, 789.
(42) Belluco, U.; Cattalini, L.; Basolo, F.; Pearson, R. G.; Turco, A. *Inorg. Chem*. **1965**, *4*, 925.
(43) Burdett, J. K. *Inorg. Chem*. **1977**, *16*, 3013.

$(H_2O)_2]$, $[PtCl(H_2O)_3]^+$, *trans*-$[PtCl_3Me_2SO]^-$, *trans*-$[PtCl_2(H_2O)Me_2SO]$, *cis*-$[PtCl(H_2O)_2\ Me_2SO]^+$, and *trans*-$[PtCl(H_2O)_2\ Me_2SO]^+$ (Figures S1−S9), correlation between the rate constant k_{lim} for the Hg^{2+}-assisted aquation and the spontaneous aquation rate constant k_{aq} (Figure S10), and UV spectra for Pt−Hg adducts (Fig S11). This material is available free of charge via the Internet at http://pubs.acs.org.

IC000320J